



# Environmental impacts of biodegradable microplastics

Received: 24 January 2024

Accepted: 4 September 2024

Published online: 27 September 2024

Check for updates

Zhengyin Piao<sup>1</sup>, Amma Asantewaa Agyei Boakye<sup>1</sup> & Yuan Yao<sup>1,2</sup>

Biodegradable plastics, perceived as 'environmentally friendly' materials, may end up in natural environments. This impact is often overlooked in the literature due to a lack of assessment methods. This study develops an integrated life cycle impact assessment methodology to assess the climate-change and aquatic-ecotoxicity impacts of biodegradable microplastics in freshwater ecosystems. Our results reveal that highly biodegradable microplastics have lower aquatic ecotoxicity but higher greenhouse gas (GHG) emissions. The extent of burden shifting depends on microplastic size and density. Plastic biodegradation in natural environments can result in higher GHG emissions than biodegradation in engineered end of life (for example, anaerobic digestion), contributing substantially to the life cycle GHG emissions of biodegradable plastics (excluding the use phase). A sensitivity analysis identified critical biodegradation rates for different plastic sizes that result in maximum GHG emissions. This work advances understanding of the environmental impacts of biodegradable plastics, providing an approach for the assessment and design of future plastics.

Plastics are essential to industrialization but pose enduring end-of-life (EoL) challenges for current and future generations<sup>1,2</sup>. Large volumes of waste plastics have accumulated in ecosystems, leading to widespread environmental burdens that have not been fully understood<sup>3–5</sup>. Multi-faceted efforts to address these challenges include developing biodegradable plastics and other alternatives<sup>6–10</sup> and quantifying material flows and environmental burdens of plastic EoL in natural environments (such as rivers and oceans)<sup>11–13</sup>. Previous analyses that assessed the future of plastic scenarios for net-zero greenhouse gas (GHG) emissions projected a high portion of bio-based but non-biodegradable plastics<sup>14–16</sup>. However, many bio-based plastics are marketed for their biodegradability (for example, poly(lactic acid) (PLA))<sup>17</sup>. In fact, more than 50% of global bio-based plastics are biodegradable, with this fraction expected to increase further in the next decade<sup>18</sup>.

Biodegradable plastics can be made from biomass or fossil fuels, and their environmental benefits remain debatable: biodegradable plastics can reduce plastic pollution such as microplastics<sup>19</sup>; however, their biodegradation results in GHG emissions during EoL processes such as landfilling<sup>20</sup>. Biogenic carbon in bio-based, biodegradable plastics adds additional complexity. Whereas some studies have

suggested that the uptake of biogenic carbon by biomass can offset some GHG emissions from plastic EoL<sup>15,16</sup>, quantitative assessments for biodegradable plastics remain lacking. To inform current debates and support sustainability decisions, a detailed understanding of the environmental impacts of both bio- and fossil-based plastics is essential. This requires a consideration of the impacts across plastic production and both engineered and non-engineered EoL pathways. Several life cycle assessment (LCA) studies have examined the environmental impacts of biodegradable plastics, but they focused only on engineered EoL pathways (for example, industrial composting and anaerobic digestion)<sup>21,22</sup>. As a result, these insights may not necessarily be generalized to biodegradable plastics that are released into natural environments where microplastics and their environmental impacts remain underexplored<sup>23</sup>.

Microplastics are often excluded from traditional LCAs due to a lack of standardized assessment methods<sup>24,25</sup>. Recent research has attempted to address this issue<sup>26–29</sup>. Some studies have proposed impact characterization factors that are designed specifically for microplastics (for example, microplastic potential or plastic pollution equivalent)<sup>26,27</sup>. However, these indicators reflect only the severity

<sup>1</sup>Center for Industrial Ecology, Yale School of the Environment, Yale University, New Haven, CT, USA. <sup>2</sup>Chemical and Environmental Engineering, Yale School of Engineering and Applied Science, Yale University, New Haven, CT, USA. e-mail: [y.yao@yale.edu](mailto:y.yao@yale.edu)

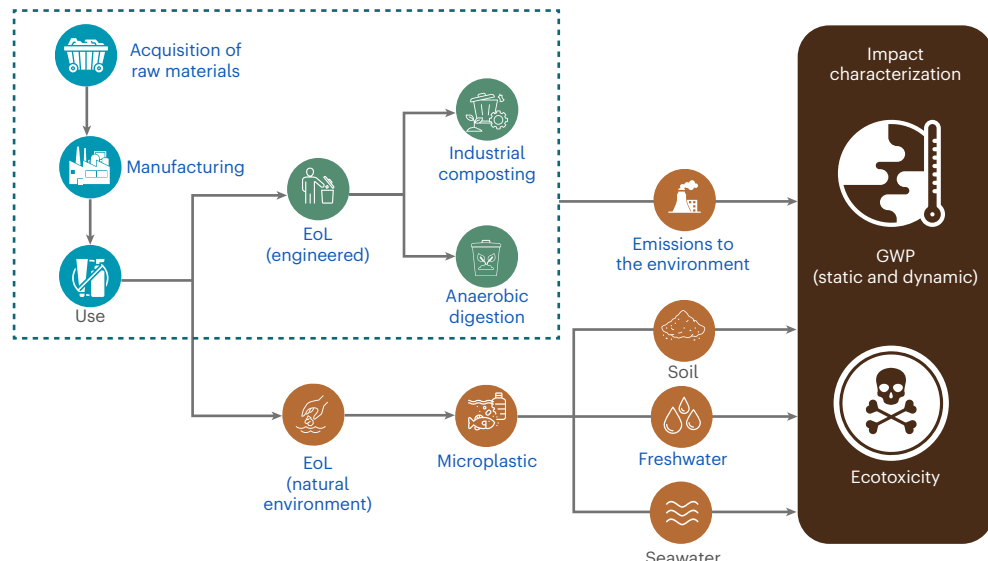


**Fig. 1 | The schematic diagram of the LCA methodology for biodegradable plastics.** Activities in blue are included in the case studies to demonstrate the LCIA methodology developed for microplastics. The dashed box shows the common system boundaries for biodegradable plastics in previous studies, including upstream production and engineered EoL.

of plastic accumulation, making them incompatible with existing methods of life cycle impact assessment (LCIA) such as ReCiPe and USEtox<sup>30,31</sup>; it is therefore not possible to perform a cradle-to-grave LCA that covers upstream production and EoL phase. Other studies have adapted existing LCIA methods such as USEtox<sup>28,29</sup>, treating microplastics as toxic particles with fate, exposure and effect factors. The output of this method aligns with common LCIA impact indicators (for example, using Comparative Toxic Units for ecotoxicity (CTUe)). However, owing to insufficient ecotoxicological data, current applications of the USEtox method to microplastics are limited to aquatic ecotoxicity, leaving other environmental impacts unexplored<sup>32</sup>. In addition, applying USEtox to biodegradable plastics is challenging due to the difficulties in linking biodegradation to fate modeling<sup>31,33</sup>.

Biodegradation is an important removal mechanism of biodegradable plastics in aquatic environments<sup>34</sup>, alongside sedimentation, as demonstrated by previous research on non-biodegradable microparticles<sup>28,35,36</sup>. Both biodegradation and sedimentation can be influenced by the properties of the microplastic such as density and size<sup>37,38</sup>. In previous studies on fate modeling, the properties of the plastic were differentiated either in sedimentation using a fixed degradation rate constant<sup>39</sup> or in biodegradation (on the basis of a specific surface degradation rate (SSDR)) using a fixed sedimentation rate constant<sup>29</sup>. These approaches simplify the dynamic interactions between biodegradation and sedimentation and how the properties of the plastic may affect such interactions, which must be addressed for a more holistic understanding of the environmental impacts of biodegradable plastics.

Here we address the research gaps as follows: we propose an integrated LCIA methodology that incorporates a modified USEtox method for the fate modeling of biodegradable microplastics. This methodology links the SSDR, density and size of microplastics to the respective rate constants for biodegradation and sedimentation, assessing the impacts of plastic EoL in natural environments. We demonstrate this methodology through case studies that assess the ecotoxicity and climate-change impacts of five biodegradable plastics, which include bio-based poly(3-hydroxybutyrate) (PHB), thermoplastic starch (TPS) and PLA, and fossil-based poly( $\epsilon$ -caprolactone) (PCL) and poly(butylene succinate) (PBS). We focus on climate change due to a lack of existing quantitative assessments but increasing concerns over GHG emissions from the EoL of biodegradable plastics<sup>20,40</sup>. Moreover, recent advancements in dynamic LCA (in contrast to traditional static

LCA methods) reveal the importance of incorporating temporal effects into carbon footprint accounting, especially for systems with time-varying GHG emissions profiles, particularly non-CO<sub>2</sub> emissions<sup>41</sup>. The GHG emissions from biodegradable plastics have temporal changes that depend on the environment and the biodegradation rate. Thus, we apply both static and dynamic LCA methods to understand the climate-change impact of these time-dependent GHG emissions, an aspect that has been previously unexplored in the literature on plastics. Finally, we assess the contribution of different EoL options to the life cycle environmental performance of biodegradable plastics, revealing the associated environmental benefits and risks. The proposed methodology can assess both existing biodegradable and non-biodegradable plastics and support the design of future plastics.

## Results

Figure 1 depicts the proposed methodology. Engineered EoL includes industrial composting and anaerobic digestion. EoL in natural environments refers to waste plastics that enter soil, marine water and freshwater ecosystems through biodegradation (GHG emissions) and microplastics (ecotoxicity). To quantify the climate impact of time-dependent GHG emissions from biodegradation, both static and dynamic global warming potential (GWP) accounting methods are included. This flexible methodology applies to various plastics in two ways. First, it starts with EoL modeling but can expand the system boundary to include other phases, such as raw material production and manufacturing, for cradle-to-grave analyses. Second, the methodology incorporates the physical properties of plastics, ecotoxicological results and biodegradation testing, which is applicable to different plastics with available experimental data. Although this paper focuses on ecotoxicity and GWP, the methodology can be adapted to assess other environmental impacts in LCAs of different plastics.

To demonstrate the methodology in Fig. 1, we conducted case studies on five biodegradable plastics that are common in the market<sup>42</sup>: bio-based PHB, TPS and PLA; and fossil-based PCL and PBS. The functional unit is 1 kg of biodegradable microplastics, with particle diameters ranging from micrometers (1,000, 100 and 10  $\mu\text{m}$ ) to nanometers (1 and 0.1  $\mu\text{m}$ ). The system boundary is cradle-to-grave, excluding the 'use phase' which varies by plastic product and requires case-by-case assessment. The presence of microplastics in these size classes in aquatic environments has been reported<sup>43</sup>. EoL modeling considers the

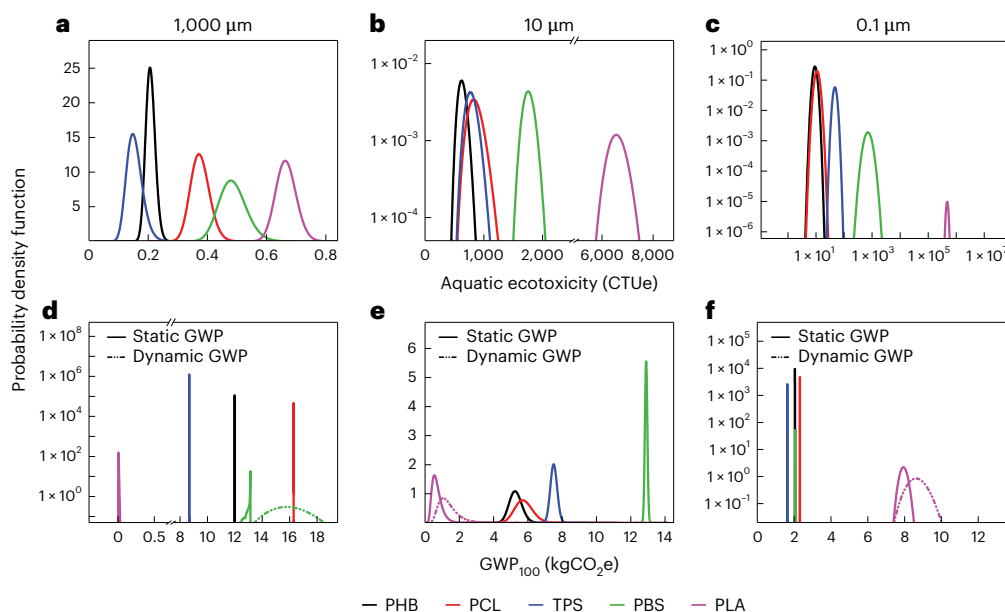


**Fig. 2 | Environmental impact measures of common biodegradable plastics with an EoL in natural environments under scenario 1.** a–f, Aquatic ecotoxicity (a–c) and GHG emission (d–f) results for three size classes of biodegradable microplastics (per kilogram). The results show the uncertainties in a freshwater ecosystem across the different size classes of 1,000  $\mu\text{m}$  (a,d), 10  $\mu\text{m}$  (b,e) and 0.1  $\mu\text{m}$  (c,f) under scenario 1 (aerobic conditions in the water and anaerobic conditions in the sediment). The GHG emissions are expressed as the 100 year GWP on the basis of static (solid lines) and dynamic (dotted lines) methods.

Dynamic GWP results are shown only for PBS and PLA in certain size classes, as the other plastics exhibit similar GWP results between the static and dynamic methods (see Supplementary Table 3). Results for additional size classes and scenarios are documented in Supplementary Sections 2.1 and 2.2. Ecotoxicological CF values are provided in Supplementary Table 2, whereas GWP values are in Supplementary Tables 3 and 4. Supplementary Section 2.4 compares these results with previous studies<sup>29</sup>.

entry of microplastics into a freshwater ecosystem, followed by their residence in water and sediment. Biodegradation occurs continuously in both water and sediment compartments over the 100 year duration of this study or until complete mineralization.

A recent review<sup>44</sup> on plastic biodegradation in aquatic environments indicates a predominance of aerobic microbes in water and anaerobic microbes in deep sediment. In shallow sediment, both aerobic and anaerobic microbes may exist, but the aerobic/anaerobic ratios have not been quantified<sup>44</sup>. To explore this uncertainty, we considered two scenarios: scenario 1 assumes aerobic conditions in water and anaerobic conditions in sediment, which is more likely; scenario 2 assumes aerobic conditions in both water and sediment, which may occur in shallow sediment. Anaerobic conditions in water are excluded as they occur only under special environmental conditions such as severe eutrophication. The GWP for 100 years (GWP<sub>100</sub>, in units of kilograms CO<sub>2</sub>-equivalent per kilogram microplastic (kgCO<sub>2</sub>e per kg MP)) is quantified on the basis of the IPCC (Intergovernmental Panel on Climate Change) guidelines<sup>45</sup>. For the environmental burdens of microplastics in aquatic environments, we applied the indicator of aquatic ecotoxicity (in units of CTUe per kg MP) from USEtox, a methodology that assesses the pollutant impact and can incorporate experimental results of new pollutants such as microplastics<sup>31,32</sup>. Our ecotoxicological characterization factor (CF) considers only the physical toxicity of microplastics, excluding the chemical toxicity due to a lack of data. Moreover, recent ecotoxicological studies on microplastics<sup>46–49</sup> have considered physical toxicity to be an important part of ecotoxicity. Thus, ‘ecotoxicity’ is used in this study but includes only physical effects.

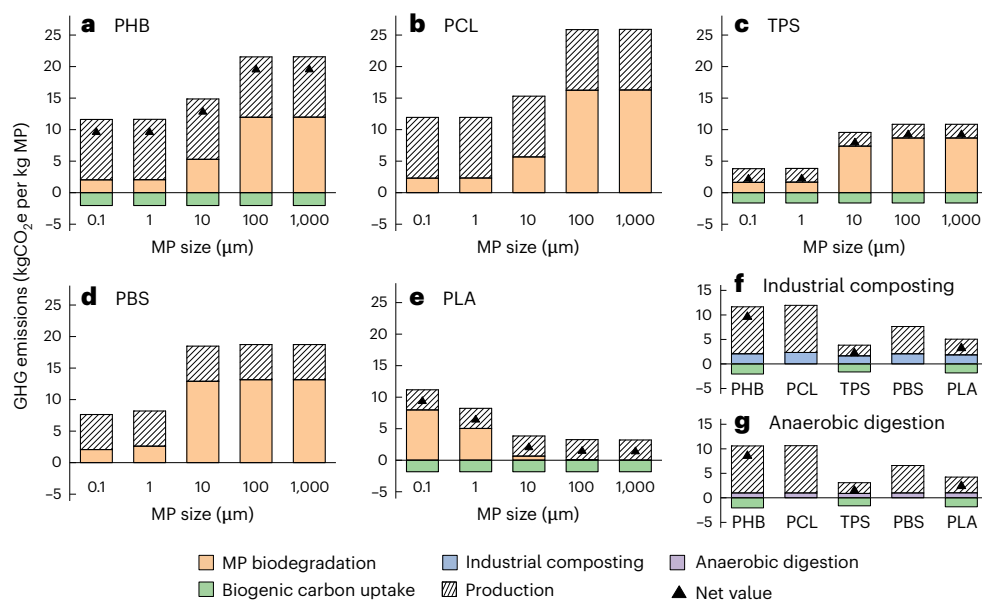
### Environmental impacts for plastic EoL in natural environments

Figure 2 shows two environmental impact measures of five biodegradable plastics with EoL in natural environments under scenario 1 for three size classes. Dynamic GWP data are shown only for PBS and PLA in certain size classes as the other plastics have similar GWP results

between the static and dynamic methods (see Supplementary Table 3). Detailed methods and parameters are given in the Methods and Supplementary Section 1. The probability density functions are determined from uncertainty analyses using Monte Carlo simulations, which consider the probability distributions of the SSDRs and densities of the five plastics. Details of the uncertainty analyses are documented in Supplementary Section 4.

Figure 2 shows the potential trade-offs between GWP and aquatic ecotoxicity. At 1,000, 100 and 10  $\mu\text{m}$  particle diameters, PLA has the lowest GWP but the highest aquatic ecotoxicity, mainly due to its lower SSDR ( $-0.001 \mu\text{m yr}^{-1}$  (ref. 27)) in freshwater and sediment than other plastics such as PHB ( $-500 \mu\text{m yr}^{-1}$  (ref. 27)). Given the low SSDR of PLA, which is similar to that of conventional plastics in aquatic environments ( $0.001 \mu\text{m yr}^{-1}$  (refs. 27,29)), our results indicate that replacing PLA or conventional plastics with biodegradable plastics, such as PHB, PCL, TPS and PBS, may shift the burden from reduced aquatic ecotoxicity to increased GWP for an EoL in aquatic environments. The extent of this burden shifting depends on the size class and GWP accounting methods. For example, at 10  $\mu\text{m}$  (Fig. 2e), the static method shows that the mean GWP of PHB ( $5.28 \text{ kgCO}_2\text{e per kg MP}$ ) is approximately 8 times as high as that for PLA ( $0.65 \text{ kgCO}_2\text{e per kg MP}$ ). Using the dynamic method, the mean GWP for PHB ( $5.28 \text{ kgCO}_2\text{e per kg MP}$ ) is only about 4 times as high as that for PLA ( $1.25 \text{ kgCO}_2\text{e per kg MP}$ ).

However, at particle diameters of 1 and 0.1  $\mu\text{m}$ , our results show no burden shifting between PLA and the other plastics. Specifically, Fig. 2 reveals that, at 0.1  $\mu\text{m}$ , PLA has the highest aquatic ecotoxicity and the highest GWP, whereas the other plastics have similar GWP results. At 0.1  $\mu\text{m}$ , all five plastics achieve full biodegradation on the basis of their SSDRs in Supplementary Table 13 (refs. 27,37). Owing to their high SSDR values, PHB, PCL, TPS and PBS show almost entire aerobic degradation in water. Around 90% of nanometer-sized PLA (0.1  $\mu\text{m}$ ) degrades anaerobically in sediment within 100 years, leading to more methane emissions and a higher GWP, whereas less than 1% of micrometer-sized PLA (1,000 and 10  $\mu\text{m}$ ) degrades anaerobically



**Fig. 3 | Breakdown of life cycle GHG emissions for common biodegradable plastics with their EoL in natural environments or engineered settings.**

**a–g**, Life cycle GHG emission result for the five plastics with EoL in a natural environment (**a–e**) and an engineered setting (**f,g**). In **a–e**, the x axes show the various microplastic sizes. In **f,g**, the two engineered EoL pathways (industrial composting and anaerobic digestion, respectively) are shown, with the x axes displaying the five different plastic types. The cradle-to-grave

LCA includes upstream production (hatched bars), biogenic carbon uptake for bio-based biodegradable plastics (green-shaded bars), and EoL in natural environments (orange-shaded bars) or engineered settings (blue- and purple-shaded bars) but excludes the use phase of the biodegradable plastics. The results in **a–e** are based on scenario 1 (that is, aerobic conditions in the water and anaerobic conditions in the sediment).

within 100 years, resulting in a lower GWP. Furthermore, as more than 99% of PHB, PCL, TPS and PBS particles degrade aerobically at 0.1  $\mu\text{m}$ , their GWP differences depend on the carbon content, with PCL being the highest and TPS the lowest. For aquatic ecotoxicity, our sensitivity analyses (Supplementary Section 8) indicate that the SSDR is the dominant factor at 1 and 0.1  $\mu\text{m}$ , with a high SSDR reducing the aquatic ecotoxicity. Consequently, PHB (with the highest SSDR) shows the lowest aquatic ecotoxicity at 0.1  $\mu\text{m}$ .

In addition to the SSDR, size and carbon content, the density of the plastic influences the environmental performance of PHB, PCL, TPS and PBS at 1,000, 100 and 10  $\mu\text{m}$ . Sensitivity analyses (Supplementary Section 8) show that the density is inversely correlated with the aquatic ecotoxicity. A high density leads to a high sedimentation velocity, reducing the residence time in water. Thus, despite TPS having a lower SSDR than PCL, its higher density results in a lower aquatic ecotoxicity at 1,000  $\mu\text{m}$ .

As plastic biodegradation is dynamic, we performed both static and dynamic GWP accounting. PHB, PCL and TPS show negligible differences between static and dynamic values across the size classes, apart from PBS at 1,000  $\mu\text{m}$  (a 20% difference; Fig. 2d) and PLA at 1  $\mu\text{m}$  (an 80% difference, as shown in Supplementary Fig. 1). To explain these results, Supplementary Figs. 4 and 5 show methane emissions every ten years with the corresponding static and dynamic GWP values for PBS (at 1,000  $\mu\text{m}$ ) and PLA (at 1  $\mu\text{m}$ ). Methane emissions from PBS and PLA last for 79 and 100 years, respectively, causing substantial differences due to the different GWP characterization factors of methane for the static and dynamic methods. By contrast, the results for PHB, PCL and TPS are close to pulse emissions, due to their fast biodegradation that emits GHGs quickly<sup>41</sup>. This indicates that a traditional static LCA may underestimate the climate-change impacts of slowly degrading biodegradable plastics at EoL.

For scenario 2, with aerobic conditions in both the water and sediment, Supplementary Fig. 2 shows that the trade-off between GWP and ecotoxicity still exists at 1,000, 100, 10 and 1  $\mu\text{m}$ , but with less burden shifting compared with scenario 1 due to the absence of

methane-releasing anaerobic biodegradation. At 0.1  $\mu\text{m}$ , no burden shifting is observed as all five plastics degrade fully within 100 years.

#### Contribution of plastic EoL to life cycle GHG emissions

This section describes the contribution of various EoL alternatives (comprising engineered EoL, which includes industrial composting and anaerobic digestion, and EoL in natural environments) to the life cycle GHG emissions of biodegradable plastics (excluding the use phase). Figure 3 presents the results of scenario 1, with life cycle inventories for the production and engineered EoL of the biodegradable plastics documented in Supplementary Section 3. Determination of the carbon uptake follows methods from previous research<sup>50–52</sup>, which modeled biogenic carbon uptake on the basis of the carbon content of plastics.

Figure 3 illustrates that GHG emissions from biodegradation in natural environments (orange bars) are either comparable or higher than emissions from engineered EoL pathways (blue and purple bars), depending on the plastic type and size class. The largest difference is observed for PCL, where emissions from biodegradation in natural environments (16.3 kgCO<sub>2</sub>e per kg MP, as shown by the orange bar for 1,000  $\mu\text{m}$  in Fig. 3b) are about 16 times those from anaerobic digestion (1.01 kgCO<sub>2</sub>e per kg MP, as shown by the purple bar for PCL in Fig. 3g). The primary reason is that anaerobic biodegradation is the main GHG source for PLA at 1 and 0.1  $\mu\text{m}$  sizes and for the other plastics at 1,000, 100 and 10  $\mu\text{m}$  in natural environments. By contrast, engineered EoL can maintain aerobic conditions through industrial composting or recover energy by capturing methane generated from anaerobic digestion. These high GHG emissions of biodegradable plastic litter in natural environments underscore the need for the proper, engineered EoL management of biodegradable plastics.

Moreover, Fig. 3 shows that the EoL of biodegradable plastics substantially contributes to their life cycle GHG emissions. In our results, EoL phases account for up to 61, 63, 94, 70 and 85% of the life cycle GHG emissions (excluding the use phase) of PHB, PCL, TPS, PBS and PLA, respectively. This study uses corn as the biomass source as it is the main feedstock for bio-based plastics (PHB, TPS and PLA)<sup>53,54</sup>.

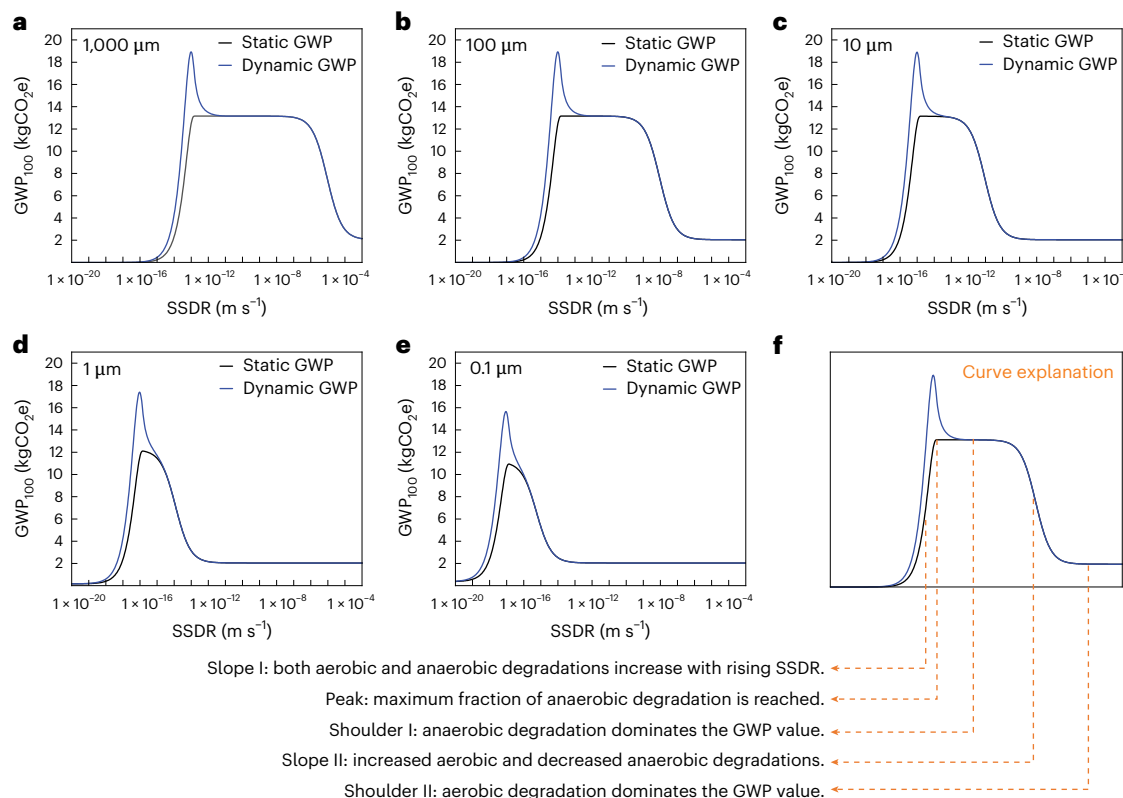


**Fig. 4 | Impact of SSDR on GHG emissions from plastic biodegradation in natural environments.** a–e, Using PBS as an example, GHG emissions (quantified as GWP) via static and dynamic methods across different size classes of 1,000 μm (a), 100 μm (b), 10 μm (c), 1 μm (d) and 0.1 μm (e) to determine the GWP for 100 years. f, Explanation of the GWP–SSDR curves.

Land use change for corn is not considered, given the minor use of corn for bio-based plastic production and the lack of relevant data, with existing literature focusing on the production of biofuels from corn<sup>55</sup>. Although previous literature reports indicate that GHGs from the engineered EoL of bio-based plastic can be offset by biogenic carbon uptake<sup>14</sup>, Fig. 3 shows that for bio-based biodegradable plastics, GHG emissions from EoL in natural environments cannot be fully offset due to methane emissions.

The results for scenario 2 are documented in Supplementary Fig. 3, which shows similar GWP values for EoL in natural environments and engineered EoL, regardless of the size class. The GWP of EoL can be partially offset by the biogenic carbon uptake of bio-based plastics in both scenarios 1 and 2 (for example, PHB, TPS and PLA). Compared with scenario 1, the GWP of EoL in natural environments is lower in scenario 2. However, scenario 2 is an extreme case that assumes only aerobic microbes in the sediment, resulting in the lower bound of GWP. If anaerobic microbes are present in the sediment, the GWP results will be higher.

### Effects of plastic properties on their EoL impacts

The results in Figs. 2 and 3 are based on the current design of biodegradable plastics, which prompts the question: how will the future design of biodegradable plastics with different SSDRs and densities affect their EoL impacts in natural environments? To explore this, we conducted sensitivity analyses with various densities and SSDRs in freshwater environments for the five plastics with different size classes, assuming a constant SSDR ratio of water to sediment. Supplementary Figures 7–11 show that increasing the plastic density increases the GWP monotonically (if microplastics biodegrade completely within 100 years) and reduces the aquatic ecotoxicity. As the SSDR increases, the aquatic ecotoxicity declines monotonically. Nevertheless, the SSDR impacts on the GWP are non-monotonic. Figure 4 illustrates that increasing

biodegradability may increase or decrease the GHG emissions at EoL in natural environments. GWP increases with SSDR until it reaches a 'peak' value (Fig. 4f), where anaerobic degradation reaches the maximum fraction (further explanation is provided in Supplementary Section 10). If the SSDR is below the rate at which anaerobic biodegradation reaches a maximum (that is, SSDR<sub>peak</sub>), improving the biodegradability increases the GWP ('slope I' in Fig. 4f). If the SSDR exceeds SSDR<sub>peak</sub>, the GWP decreases ('slope II' in Fig. 4f). In addition, GWP is insensitive to the SSDR when either anaerobic ('shoulder I') or aerobic degradation ('shoulder II') dominates. Therefore, there is no universal rule that a higher or lower biodegradability is better for plastic EoL in terms of climate impact (as assessed here).

Our analysis method can guide engineers in designing low-carbon biodegradable plastics, especially for primary microplastics with designated particle sizes, such as microplastic applications in cleaning and cosmetic products. Engineers can measure the density, SSDR and biodegradation products (for example, CO<sub>2</sub> and methane) of new plastics experimentally. Using these data and this method, they can generate the GWP–SSDR curve and pinpoint the critical SSDR at different microplastic sizes. By comparing the measured SSDR with the critical SSDR, engineers can assess the risk of high GWP in natural environments and design lower-carbon-footprint biodegradable plastics by adjusting the particle size, degradation performance or carbon content as needed. Supplementary Section 6 provides further details in the design of new plastics.

Figure 4 also shows that the sensitivity of GWP to SSDR depends on the size class. For smaller sizes, the GWP is more affected by a lower SSDR, whereas it becomes less sensitive at a higher SSDR, as shown by the increasing length of shoulder II in Figs. 4a–e. This provides engineers with a powerful approach to estimate the climate impact of biodegradable plastics on the basis of size characteristics. Moreover, Fig. 4 presents the static and dynamic GWP results as separate lines.

For each size class, the two lines overlap as the SSDR increases to a specific value. The differences between the static and dynamic GWP results at low SSDR are caused mainly by methane emissions from anaerobic degradation. The static method tends to underestimate the GWP for low-SSDR plastics with time-varying methane emissions, which is consistent with previous dynamic LCA findings<sup>41</sup>. This suggests that dynamic methods should be used to quantify the GWP at EoL for plastics with a low SSDR, regardless of the size class.

## Discussion

This study presents an integrated LCA methodology for assessing the environmental impacts of biodegradable plastics. Case studies of five common plastics demonstrate that faster biodegradation (for example, for PHB, PCL, TPS and PBS) may shift the burden from reduced ecotoxicity to increased climate impact at EoL in natural environments. Our results identify the size class as a critical factor in determining the extent of burden shifting, an aspect that has not been focused on in previous LCA studies<sup>21,22</sup>. Our results indicate that plastic biodegradation in natural environments can lead to higher GHG emissions than biodegradation via engineered EoL. This emphasizes the importance of the proper EoL management of biodegradable plastics, which requires suitable infrastructure.

We demonstrated that the EoL of plastic in natural environments can substantially contribute to life cycle GHG emissions (excluding the use phase) and cannot be fully offset by biogenic carbon uptake. Therefore, generic LCAs of plastics may largely underestimate the environmental burdens of biodegradable plastics, especially in natural environments. Our sensitivity analyses show that increasing the plastic biodegradability can either increase or decrease the GHG emissions at EoL, depending on the  $SSDR_{peak}$  value. This method can guide the design of future plastics via identifying  $SSDR_{peak}$  and developing low-carbon biodegradable plastics from a life cycle perspective.

Our results also show that the traditional static GWP accounting method tends to underestimate the potential climate-change impacts of the EoL of plastics with low biodegradability, which slowly releases methane from anaerobic degradation. Dynamic GWP accounting should be considered for plastics with low biodegradability. This method can also be applied to conventional plastics to quantify their EoL impacts in natural environments. Supplementary Section 7 includes an additional case study on the non-biodegradable plastic polyethylene terephthalate, one of the most widely produced plastics, using our methodology.

This study has a few limitations. The SSDR data for the five plastics were based on a previous review<sup>27</sup> of 38 experimental datasets (details in Supplementary Section 5), which may vary in experimental conditions. This does not affect the applicability of our methodology, which can analyse plastics using primary data from specific biodegradation tests. Our study adapted freshwater ecosystem parameters from USEtox considering the global landscape, which should be adjusted to local conditions for region-specific analyses. In addition, this study only includes the physical toxicity of microplastics and excludes chemical toxicity, which is still in the early stages of research. The use phase was excluded due to a lack of data on microplastics generation, a common limitation in previous LCAs of biodegradable plastics<sup>56</sup>. Future research should improve the modeling and data for the fragmentation of macroplastics into microplastics, which is the foundation for assessing the generation of microplastics throughout the life cycle of plastics. Microplastic generations are important life cycle inventory data that can be combined with the LCIA characterization factors developed in this study for aquatic ecotoxicity and GWP (as presented in Supplementary Tables 2–4) to conduct comprehensive LCA for various plastics. Factors such as plastic types, pre-processing and environmental elements (for instance, ultraviolet light) influence plastic fragmentation, meaning that more data and modeling are required to fully understand and quantify their impacts on plastic breakdown<sup>57–61</sup>. Fragmentation can

be integrated into our methodology once sufficient data and models are available, enabling comprehensive assessments of microplastic generation in life cycle inventory analysis and their environmental impacts in LCAs.

Our fate modeling excludes biofouling due to a lack of methods and data with which to quantify its effects on plastic densities and attachment efficiencies. High-density microplastics typically reach sediment before biofouling acceleration<sup>62</sup>. Thus, our method applies directly to high-density plastics (for example, those analysed in this study) that sink without biofouling. For low-density plastics, our method is applicable if biofouling-based densities and attachment efficiencies can be quantified. Our LCIA method does not include species in the sediment, similar to other LCIA methods (for example, ReCiPe, TRACI and USEtox)<sup>30,31,63</sup>, due to a richer species presence in water and a lack of ecotoxicological data for sediment species. Future research should fill these data gaps, enabling integration into our method. We demonstrated our methodology in a freshwater ecosystem. Future research should explore diverse natural environments such as soil/groundwater and marine water/sediment ecosystems.

## Methods

The method of this research aims to quantify the aquatic ecotoxicity and GHG emissions that result from the entry of biodegradable microplastics into a freshwater ecosystem. The first step is to perform the fate modeling to determine the fate factors of plastics in water ( $FF_{w,w}$  (day)), sediment ( $FF_{s,s}$  (day)) and from water to sediment ( $FF_{s,w}$  (day)). The fate factor in water ( $FF_{w,w}$ ) is applied to quantify the aquatic ecotoxicity (CF (in units of CTUe per kg MP)). The fate factors in sediment ( $FF_{s,s}$ ) and from water to sediment ( $FF_{s,w}$ ) derive the mass fraction of plastic sedimentation. This is then used to determine the fractions of aerobic and anaerobic biodegradation for calculating the GWP of GHG emissions in 100 years (expressed as  $GWP_{100}$ ).

### Aquatic ecotoxicity

Equation (1)<sup>31,64</sup> shows the overarching calculation of aquatic ecotoxicity (CF), which consists of the fate factor in water ( $FF_{w,w}$ ), the exposure factor (XF) and the effect factor (EF (measured in units of PAF m<sup>3</sup> per kg MP, where PAF denotes the potentially affected fraction of species)):

$$CF = FF_{w,w} \times XF \times EF. \quad (1)$$

$FF_{w,w}$  is derived from the fate modeling. The values of XF and EF are listed in Supplementary Table 1.

### Greenhouse gas emissions

Equation (2) shows the calculation of GHG emissions quantified using  $GWP_{100}$ :

$$GWP_{100} = GWP_{100,w} + GWP_{100,s} \quad (2)$$

where  $GWP_{100,w}$  and  $GWP_{100,s}$  are the 100 year GWP values due to the biodegradation of plastics in water and sediment, respectively. Their calculations are shown in Equations (3) and (4):

$$GWP_{100,w} = M_{CO_2,w}^{\text{theoretical}} \times WL_w \times w_{CO_2} \quad (3)$$

$$GWP_{100,s} = \sum_{t=1}^{100} \sum_{GHG} (M_{GHG,s}^{\text{theoretical}} \times WL_{t,s} \times w_{GHG,t}) \quad (4)$$

where  $M_{CO_2,w}^{\text{theoretical}}$  (measured in kgCO<sub>2</sub> per kg MP) is the theoretical amount of CO<sub>2</sub> from the complete biodegradation of plastics in water and  $M_{GHG,s}^{\text{theoretical}}$  (measured in kg GHG per kg MP) is the theoretical amount of GHG (including CO<sub>2</sub> and methane) generated from the

complete biodegradation of plastics in sediment. The calculations of  $M_{CO_2,w}^{theoretical}$  and  $M_{GHG,s}^{theoretical}$  are explained further in Supplementary Equations (1), (3) and (4). Variable  $WL_w$  is the fraction of mass loss due to the biodegradation in water, and  $WL_{ts}$  is the fraction of mass loss due to the biodegradation in sediment at time  $t$  (measured in years). In this study, we introduced the SSDR and fate factors  $FF_{s,w}$  and  $FF_{s,s}$  to derive  $WL_w$  and  $WL_{ts}$ , with detailed calculations shown in Supplementary Equations (2) and (5)–(7).

Variable  $w_{CO_2}$  (measured in kgCO<sub>2</sub>e per kgCO<sub>2</sub>) is the GWP per kilogram of CO<sub>2</sub>, which is 1 by definition as CO<sub>2</sub> is the reference substance<sup>45</sup>. The parameter  $w_{GHG,t}$  (measured in kgCO<sub>2</sub>e per kg GHG) is the GWP per kilogram of GHG (including CO<sub>2</sub> and methane) at time  $t$  and is related to the static and dynamic calculations of this study. For the static method, we applied a constant value of  $t$  (that is, 100 years). For the dynamic method, we considered different GWP factors for emissions at different  $t$  values. Supplementary Equation (8) shows the details for calculating  $w_{GHG,t}$ .

### Fate modeling

On the basis of the USEtox methodology, the overall result of the fate modeling is the fate matrix (FF) derived from equation (5)<sup>31,64</sup>:

$$\bar{FF} = \begin{pmatrix} FF_{w,w} & FF_{w,s} \\ FF_{s,w} & FF_{s,s} \end{pmatrix} = -\bar{k}^{-1} \quad (5)$$

where  $FF_{w,w}$ ,  $FF_{s,s}$  and  $FF_{s,w}$  are defined as above,  $FF_{w,s}$  (also measured in days) denotes the fate factor of plastics from sediment to water and  $\bar{k}$  (s<sup>-1</sup>) is the rate constant derived from equation (6)<sup>31,64</sup>:

$$\bar{k} = \begin{pmatrix} -k_{w,w} & k_{w,s} \\ k_{s,w} & -k_{s,s} \end{pmatrix} \quad (6)$$

Here,  $k_{w,w}$ ,  $k_{s,s}$ ,  $k_{w,s}$  and  $k_{s,w}$  denote the rate constants in water, sediment, from sediment to water and from water to sediment, respectively (all with units of s<sup>-1</sup>). Equations (7)–(10) show the calculations of the four rate constants:

$$k_{w,w} = k_{deg,w} + k_{sed} + k_{adv} \quad (7)$$

$$k_{s,w} = k_{sed} \quad (8)$$

$$k_{s,s} = k_{deg,s} + k_{sed,transfer} + k_{burial} + k_{resusp} \quad (9)$$

$$k_{w,s} = k_{resusp} \quad (10)$$

In the water compartment, we considered biodegradation ( $k_{deg,w}$  (s<sup>-1</sup>)), sedimentation ( $k_{sed}$  (s<sup>-1</sup>)) and advection ( $k_{adv}$  (s<sup>-1</sup>)) as the removal mechanisms of biodegradable plastics. We applied the SSDR and the diameter of the plastic particles to include biodegradation in the fate modeling (Supplementary Equation (9)). Sedimentation is another major removal mechanism. In this research,  $k_{sed}$  is derived from a sedimentation model that includes the settling of a single plastic particle (Supplementary Equations (10)–(12)) and the homo-aggregation (Supplementary Equations (10) and (13)–(19)) and hetero-aggregation (Supplementary Equations (10) and (20)–(26)) of plastic particles. The sedimentation model differentiates the density and size of the plastics. This helps to relate the physical properties of different plastics to their fate factors. The advection rate constant ( $k_{adv}$ ) depends on the flow rate and volume of freshwater, as calculated using Supplementary Equation (27).

In the sediment compartment, we incorporated four removal mechanisms (biodegradation, sediment transfer, burial and resuspension) of plastics into the fate modeling. Calculation of the biodegradation rate constant in sediment ( $k_{deg,s}$  (s<sup>-1</sup>)) is the same as that in the water compartment (Supplementary Equation (28)). Considering

biodegradation in sediment is not only important for calculating the fate factors but is also necessary for estimating the emissions of methane. The rate constants of sedimentation transfer ( $k_{sed,transfer}$  (s<sup>-1</sup>)) and resuspension ( $k_{resusp}$  (s<sup>-1</sup>)) are calculated using Supplementary Equations (29) and (30), respectively. The burial rate constant ( $k_{burial}$  (s<sup>-1</sup>)) is based on the value from the literature, as listed in Supplementary Table 1.

### Data availability

All relevant data that support the findings of this research are available within the Article and its Supplementary Information. The life cycle inventory data of the upstream production of materials and energy inputs for producing and disposing of biodegradable plastics are from the ecoinvent database (<https://ecoinvent.org/>), which requires a license for its access.

### References

1. On the plastics crisis. *Nat. Sustain.* **6**, 1137 (2023).
2. Lau, W. W. Y. et al. Evaluating scenarios toward zero plastic pollution. *Science* **369**, 1455–1461 (2020).
3. Borrelle, S. B. et al. Predicted growth in plastic waste exceeds efforts to mitigate plastic pollution. *Science* **369**, 1515–1518 (2020).
4. Horton, A. A. Plastic pollution: when do we know enough? *J. Hazard. Mater.* **422**, 126885 (2022).
5. MacLeod, M., Arp, H. P. H., Tekman, M. B. & Jahnke, A. The global threat from plastic pollution. *Science* **373**, 61–65 (2021).
6. Hunt, C. F., Lin, W. H. & Voulvouli, N. Evaluating alternatives to plastic microbeads in cosmetics. *Nat. Sustain.* **4**, 366–372 (2021).
7. Lahiri, S. K., Azimi Dijvejin, Z. & Golovin, K. Polydimethylsiloxane-coated textiles with minimized microplastic pollution. *Nat. Sustain.* **6**, 559–567 (2023).
8. Sternberg, J. & Pilla, S. Chemical recycling of a lignin-based non-isocyanate polyurethane foam. *Nat. Sustain.* **6**, 316–324 (2023).
9. Xia, Q. et al. A strong, biodegradable and recyclable lignocellulosic bioplastic. *Nat. Sustain.* **4**, 627–635 (2021).
10. Duraj-Thatte, A. M. et al. Water-processable, biodegradable and coatable aquaplastic from engineered biofilms. *Nat. Chem. Biol.* **17**, 732–738 (2021).
11. Gontard, N., David, G., Guilbert, A. & Sohn, J. Recognizing the long-term impacts of plastic particles for preventing distortion in decision-making. *Nat. Sustain.* **5**, 472–478 (2022).
12. González-Fernández, D. et al. Floating macrolitter leaked from Europe into the ocean. *Nat. Sustain.* **4**, 474–483 (2021).
13. Woodward, J., Li, J., Rothwell, J. & Hurley, R. Acute riverine microplastic contamination due to avoidable releases of untreated wastewater. *Nat. Sustain.* **4**, 793–802 (2021).
14. Bachmann, M. et al. Towards circular plastics within planetary boundaries. *Nat. Sustain.* **6**, 599–610 (2023).
15. Meys, R. et al. Achieving net-zero greenhouse gas emission plastics by a circular carbon economy. *Science* **374**, 71–76 (2021).
16. Stegmann, P., Daioglou, V., Londo, M., van Vuuren, D. P. & Junginger, M. Plastic futures and their CO<sub>2</sub> emissions. *Nature* **612**, 272–276 (2022).
17. Filiciotto, L. & Rothenberg, G. Biodegradable plastics: standards, policies, and impacts. *ChemSusChem* **14**, 56–72 (2021).
18. Bioplastics market development update 2022 European Bioplastics (2022).
19. Ghosh, K. & Jones, B. H. Roadmap to biodegradable plastics—current state and research needs. *ACS Sustain. Chem. Eng.* **9**, 6170–6187 (2021).
20. Van Roijen, E. C. & Miller, S. A. A review of bioplastics at end-of-life: linking experimental biodegradation studies and life cycle impact assessments. *Resour. Conserv. Recycl.* **181**, 106236 (2022).

21. García-Depraect, O. et al. Inspired by nature: microbial production, degradation and valorization of biodegradable bioplastics for life-cycle-engineered products. *Biotechnol. Adv.* **53**, 107772 (2021).

22. Cazaudehore, G. et al. Can anaerobic digestion be a suitable end-of-life scenario for biodegradable plastics? A critical review of the current situation, hurdles, and challenges. *Biotechnol. Adv.* **56**, 107916 (2022).

23. Wei, X.-F., Bohlén, M., Lindblad, C., Hedenqvist, M. & Hakonen, A. Microplastics generated from a biodegradable plastic in freshwater and seawater. *Water Res.* **198**, 117123 (2021).

24. Askham, C. et al. Generating environmental sampling and testing data for micro- and nanoplastics for use in life cycle impact assessment. *Sci. Total Environ.* **859**, 160038 (2023).

25. Rosenboom, J.-G., Langer, R. & Traverso, G. Bioplastics for a circular economy. *Nat. Rev. Mater.* **7**, 117–137 (2022).

26. Saling, P., Gyuzeleva, L., Wittstock, K., Wessolowski, V. & Griesshammer, R. Life cycle impact assessment of microplastics as one component of marine plastic debris. *Int. J. Life Cycle Assess.* **25**, 2008–2026 (2020).

27. Maga, D. et al. Methodology to address potential impacts of plastic emissions in life cycle assessment. *Int. J. Life Cycle Assess.* **27**, 469–491 (2022).

28. Zhao, X. & You, F. Life cycle assessment of microplastics reveals their greater environmental hazards than mismanaged polymer waste losses. *Environ. Sci. Technol.* **56**, 11780–11797 (2022).

29. Corella-Puertas, E., Hajjar, C., Lavoie, J. & Boulay, A.-M. MarILCA characterization factors for microplastic impacts in life cycle assessment: physical effects on biota from emissions to aquatic environments. *J. Clean. Prod.* **418**, 138197 (2023).

30. Lavoie, J., Boulay, A.-M. & Bulle, C. Aquatic micro- and nanoplastics in life cycle assessment: development of an effect factor for the quantification of their physical impact on biota. *J. Ind. Ecol.* **26**, 2123–2135 (2022).

31. Rosenbaum, R. K. et al. USEtox—the UNEP-SETAC toxicity model: recommended characterisation factors for human toxicity and freshwater ecotoxicity in life cycle impact assessment. *Int. J. Life Cycle Assess.* **13**, 532–546 (2008).

32. Woods, J. S., Verones, F., Jolliet, O., Vázquez-Rowe, I. & Boulay, A.-M. A framework for the assessment of marine litter impacts in life cycle impact assessment. *Ecol. Indic.* **129**, 107918 (2021).

33. Narancic, T. et al. Biodegradable plastic blends create new possibilities for end-of-life management of plastics but they are not a panacea for plastic pollution. *Environ. Sci. Technol.* **52**, 10441–10452 (2018).

34. Pu, Y., Tang, F., Adam, P.-M., Laratte, B. & Ionescu, R. E. Fate and characterization factors of nanoparticles in seventeen subcontinental freshwaters: a case study on copper nanoparticles. *Environ. Sci. Technol.* **50**, 9370–9379 (2016).

35. Praetorius, A., Scheringer, M. & Hungerbühler, K. Development of environmental fate models for engineered nanoparticles—a case study of TiO<sub>2</sub> nanoparticles in the Rhine River. *Environ. Sci. Technol.* **46**, 6705–6713 (2012).

36. Chamas, A. et al. Degradation rates of plastics in the environment. *ACS Sustain. Chem. Eng.* **8**, 3494–3511 (2020).

37. Quik, J. T. K., de Klein, J. J. M. & Koelmans, A. A. Spatially explicit fate modelling of nanomaterials in natural waters. *Water Res.* **80**, 200–208 (2015).

38. Besseling, E., Quik, J. T. K., Sun, M. & Koelmans, A. A. Fate of nano- and microplastic in freshwater systems: a modeling study. *Environ. Pollut.* **220**, 540–548 (2017).

39. Rossi, V. et al. Life cycle assessment of end-of-life options for two biodegradable packaging materials: sound application of the European waste hierarchy. *J. Clean. Prod.* **86**, 132–145 (2015).

40. Lan, K. & Yao, Y. Dynamic life cycle assessment of energy technologies under different greenhouse gas concentration pathways. *Environ. Sci. Technol.* **56**, 1395–1404 (2022).

41. Kim, M. S. et al. A review of biodegradable plastics: chemistry, applications, properties, and future research needs. *Chem. Rev.* **123**, 9915–9939 (2023).

42. Mitrano, D. M., Wick, P. & Nowack, B. Placing nanoplastics in the context of global plastic pollution. *Nat. Nanotechnol.* **16**, 491–500 (2021).

43. Wu, X. et al. Critical effect of biodegradation on long-term microplastic weathering in sediment environments: a systematic review. *J. Hazard. Mater.* **437**, 129287 (2022).

44. Forster, P. et al. in *Climate Change 2021: The Physical Science Basis* (eds Masson-Delmotte, V. et al.) 923–1054 (IPCC, Cambridge Univ. Press, 2021).

45. Choi, D. et al. In vitro chemical and physical toxicities of polystyrene microfragments in human-derived cells. *J. Hazard. Mater.* **400**, 123308 (2020).

46. Ding, R., Tong, L. & Zhang, W. Microplastics in freshwater environments: sources, fates and toxicity. *Water Air Soil Pollut.* **232**, 181 (2021).

47. Saud, S., Yang, A., Jiang, Z., Ning, D. & Fahad, S. New insights into the environmental behavior and ecological toxicity of microplastics. *J. Hazard. Mater. Adv.* **10**, 100298 (2023).

48. Thacharodi, A. et al. Microplastics in the environment: a critical overview on its fate, toxicity, implications, management, and bioremediation strategies. *J. Environ. Manage.* **349**, 119433 (2024).

49. Kim, T., Bhatt, A., Tao, L. & Benavides, P. T. Life cycle analysis of polylactic acids from different wet waste feedstocks. *J. Clean. Prod.* **380**, 135110 (2022).

50. Posen, I. D., Jaramillo, P. & Griffin, W. M. Uncertainty in the life cycle greenhouse gas emissions from US production of three biobased polymer families. *Environ. Sci. Technol.* **50**, 2846–2858 (2016).

51. Zheng, J. & Suh, S. Strategies to reduce the global carbon footprint of plastics. *Nat. Clim. Chang.* **9**, 374–378 (2019).

52. Chaudhary, V., Thakur, N., Chaudhary, S. & Bangar, S. P. in *Advances in Food and Nutrition Research* Vol. 103 (ed. Özogul, F.) 397–442 (Academic, 2023).

53. Hao, L. et al. Feasibility of biodegradable material polylactic acid as a substitute for polypropylene for disposable medical masks production verified by life cycle assessment. *J. Clean. Prod.* **448**, 141492 (2024).

54. National Academies of Sciences Engineering and Medicine. *Current Methods for Life-Cycle Analyses of Low-Carbon Transportation Fuels in the United States* (The National Academies Press, 2022).

55. Molina-Besch, K. Use phase and end-of-life modeling of biobased biodegradable plastics in life cycle assessment: a review. *Clean Technol. Environ. Policy* **24**, 3253–3272 (2022).

56. Julienne, F., Lagarde, F. & Delorme, N. Influence of the crystalline structure on the fragmentation of weathered polyolefins. *Polym. Degrad. Stab.* **170**, 109012 (2019).

57. Julienne, F., Lagarde, F., Bardeau, J.-F. & Delorme, N. Thin polyethylene (LDPE) films with controlled crystalline morphology for studying plastic weathering and microplastic generation. *Polym. Degrad. Stab.* **195**, 109791 (2022).

58. Liao, J. & Chen, Q. Biodegradable plastics in the air and soil environment: low degradation rate and high microplastics formation. *J. Hazard. Mater.* **418**, 126329 (2021).

59. Bao, R. et al. Secondary microplastics formation and colonized microorganisms on the surface of conventional and degradable plastic granules during long-term UV aging in various environmental media. *J. Hazard. Mater.* **439**, 129686 (2022).

60. Born, M. P., Brüll, C. & Schüttrumpf, H. Implications of a new test facility for fragmentation investigations on virgin (micro)plastics. *Environ. Sci. Technol.* **57**, 10393–10403 (2023).

61. Kaiser, D., Kowalski, N. & Waniek, J. J. Effects of biofouling on the sinking behavior of microplastics. *Environ. Res. Lett.* **12**, 124003 (2017).
62. Bare, J. TRACI 2.0: the tool for the reduction and assessment of chemical and other environmental impacts 2.0. *Clean Technol. Environ. Policy* **13**, 687–696 (2011).
63. Huijbregts, M. A. J. et al. ReCiPe2016: a harmonised life cycle impact assessment method at midpoint and endpoint level. *Int. J. Life Cycle Assess.* **22**, 138–147 (2017).
64. Rosenbaum, R. K., Margni, M. & Jolliet, O. A flexible matrix algebra framework for the multimedia multipathway modeling of emission to impacts. *Environ. Int.* **33**, 624–634 (2007).

## Acknowledgements

We thank the funding support from Yale University (Z.P., A.A.A.B. and Y.Y.) and the US National Science Foundation (Y.Y. and Z.P.). This work is partially supported by the National Science Foundation under grant no. 2134664. Any opinions, findings, and conclusions or recommendations expressed in this material are those of the author(s) and do not necessarily reflect the views of the National Science Foundation.

## Author contributions

Y.Y. conceived the research idea. Z.P. and Y.Y. designed the study procedure. Z.P. conducted the modeling and uncertainty analysis. Z.P. and A.A.A.B. collected and compiled the data. Z.P. and Y.Y. analysed the results. All the authors contributed to writing and editing the paper.

## Competing interests

The authors declare no competing interests.

## Additional information

**Supplementary information** The online version contains supplementary material available at <https://doi.org/10.1038/s44286-024-00127-0>.

**Correspondence and requests for materials** should be addressed to Yuan Yao.

**Peer review information** *Nature Chemical Engineering* thanks Corinne Scown, Sangwon Suh, Yvonne van der Meer and the other, anonymous, reviewer for their contribution to the peer review of this work.

**Reprints and permissions information** is available at [www.nature.com/reprints](http://www.nature.com/reprints).

**Publisher's note** Springer Nature remains neutral with regard to jurisdictional claims in published maps and institutional affiliations.

**Open Access** This article is licensed under a Creative Commons Attribution 4.0 International License, which permits use, sharing, adaptation, distribution and reproduction in any medium or format, as long as you give appropriate credit to the original author(s) and the source, provide a link to the Creative Commons licence, and indicate if changes were made. The images or other third party material in this article are included in the article's Creative Commons licence, unless indicated otherwise in a credit line to the material. If material is not included in the article's Creative Commons licence and your intended use is not permitted by statutory regulation or exceeds the permitted use, you will need to obtain permission directly from the copyright holder. To view a copy of this licence, visit <http://creativecommons.org/licenses/by/4.0/>.

© The Author(s) 2024